

# Crosslinking poly(1-trimethylsilyl-1-propyne) and its effect on solvent resistance and transport properties

Scott D. Kelman<sup>a</sup>, Scott Matteucci<sup>a</sup>, Christopher W. Bielawski<sup>b</sup>, B.D. Freeman<sup>a,\*</sup>

<sup>a</sup> Center for Energy and Environmental Resources, Department of Chemical Engineering, The University of Texas at Austin, 10100 Burnet Road, Building 133, Austin, TX 78758, United States

<sup>b</sup> Department of Chemistry and Biochemistry, The University of Texas at Austin, Austin, TX 78712, United States

Received 30 July 2007; received in revised form 29 August 2007; accepted 30 August 2007

Available online 6 September 2007

## Abstract

Poly(1-trimethylsilyl-1-propyne) (PTMSP) has been crosslinked using 3,3'-diazidodiphenylsulfone to improve its solvent resistance. This study reports the influence of crosslinker content on the solubility properties of PTMSP, its density, and its gas sorption and transport properties. Crosslinking PTMSP renders it insoluble even in excellent solvents for the uncrosslinked polymer. Gas permeability and fractional free volume (FFV) decreased as crosslinker content increased, while gas sorption was unaffected by crosslinking. Therefore, the reduction in permeability upon crosslinking PTMSP was due to decreases in diffusion coefficients. Permeability reductions due to crosslinking could be offset by adding nanoparticles to the films. The addition of 30 wt.% fumed silica nanoparticles increased the permeability of crosslinked PTMSP by approximately 80%. In mixed gas permeation experiments, when the composition of the feed gas was 98 mol% CH<sub>4</sub> and 2 mol% *n*-C<sub>4</sub>H<sub>10</sub>, uncrosslinked PTMSP had an *n*-C<sub>4</sub>H<sub>10</sub>/CH<sub>4</sub> selectivity of 31 and an *n*-C<sub>4</sub>H<sub>10</sub> permeability of 114,000 barrers at 35 °C and 14 atm feed fugacity. At the same conditions, crosslinked PTMSP containing 5 wt.% crosslinker had an *n*-C<sub>4</sub>H<sub>10</sub>/CH<sub>4</sub> selectivity of 28 and an *n*-C<sub>4</sub>H<sub>10</sub> permeability of 73,000 barrers, and crosslinked PTMSP containing 5 wt.% crosslinker and 30 wt.% fumed silica nanoparticles had an *n*-C<sub>4</sub>H<sub>10</sub>/CH<sub>4</sub> selectivity of 21 and an *n*-C<sub>4</sub>H<sub>10</sub> permeability of 110,000 barrers.

© 2007 Published by Elsevier Ltd.

**Keywords:** PTMSP; Crosslinking; Permeability

## 1. Introduction

PTMSP is the most permeable polymer known [1,2]. It is a stiff chain, high free volume glassy polymer [2]. The high permeability of PTMSP is attributed in part to its exceptionally high fractional free volume (FFV) [3] of 0.29 [4], which is believed to be a consequence of the rigid, but disordered chain conformation and low cohesive energy density [5]. High free volume polymers are often weakly size-sieving and, consequently, they are more permeable to large gas or vapor molecules than to smaller molecules. In this regard, PTMSP has outstanding vapor/gas selectivity [6–9]. For

example, the *n*-C<sub>4</sub>H<sub>10</sub>/CH<sub>4</sub> mixed gas selectivity is 35 at 25 °C, which is very high [10], and this property makes PTMSP an interesting material for reverse-selective gas separations such as volatile organic compound (VOC) removal from permanent gas streams, natural gas dewpointing, and monomer recovery from the exhaust of polymerization reactors [8,9].

However, the solvent resistance and physical stability of PTMSP needs to be improved. The solvent resistance of PTMSP is low, and it is soluble in a wide range of organic solvents [11], including both aliphatic and aromatic compounds similar to those that might be found in feed streams of interest. This high solubility compromises the utility of PTMSP in some of the applications mentioned earlier [10]. Due to the glassy nature of PTMSP, it is an inherently unstable material. The permeability of PTMSP to gases and vapors decreases

\* Corresponding author. Tel.: +1 512 232 2803; fax: +1 512 232 2807.

E-mail address: [freeman@che.utexas.edu](mailto:freeman@che.utexas.edu) (B.D. Freeman).

over time due to physical aging, which is the gradual relaxation of nonequilibrium excess free volume [7,12–18].

To improve its stability, PTMSP has been chemically and physically modified using various strategies. For example, PTMSP has been blended with rubbery polymers [16], brominated [19–22], had nanoparticles added to it [10,23], and has been crosslinked [24–26]. Crosslinking PTMSP with bis-(azide)s has previously been reported to increase both solvent resistance and physical stability [24–26]. Crosslinked PTMSP films were insoluble in common PTMSP solvents such as toluene, and the permeability of the crosslinked films was reported to be constant over time [24–26].

The crosslinking reaction described in this report capitalized on the ability of aryl azides (R–N<sub>3</sub>) to decompose to molecular nitrogen (N<sub>2</sub>) and reactive nitrenes (R–N) at elevated temperatures. Nitrenes readily add to alkenes to form three-membered heterocycles, known as aziridines, or insert into carbon–hydrogen bonds to form substituted amines [27]. Since the azide decomposition reaction cleanly generates nitrogen gas and reactive nitrene intermediates as its exclusive products, bis-(azide)s are ideal for crosslinking PTMSP because no low volatility, low molecular weight byproducts are formed that could contaminate the polymer [25].

Although previous studies have shown that custom-made bis-(azide)s and azide-functionalized polymers are effective for increasing stability of PTMSP [24–26], alkyl and carboxyl nitrenes tend to undergo intramolecular rearrangements which reduce opportunities for bimolecular crosslinking reactions [28]. In this paper, the effect of using 3,3'-diazidodiphenylsulfone, a commercially available bis(aryl azide), to crosslink PTMSP is reported. The solvent resistance of the resulting crosslinked PTMSP is examined. The permeability, solubility and diffusivity of N<sub>2</sub>, O<sub>2</sub>, CH<sub>4</sub>, C<sub>2</sub>H<sub>6</sub>, C<sub>3</sub>H<sub>8</sub> and *n*-C<sub>4</sub>H<sub>10</sub> in crosslinked PTMSP are reported, and these transport properties are correlated with the FFV of crosslinked PTMSP. The effect of nanoparticle addition on crosslinked PTMSP transport properties was also investigated. The vapor/gas mixture separation properties of uncrosslinked PTMSP and crosslinked PTMSP were determined to complement and expand upon the initial reports by Jia and Baker and Rudd et al. [25,26], which describe pure gas permeation properties of crosslinked PTMSP.

### 1.1. Theory

The permeability of a polymer film to gas A,  $P_A$ , is defined as follows [29,30]:

$$P_A = \frac{N_A \cdot l}{f_{2,A} - f_{1,A}} \quad (1)$$

where  $N_A$  is the steady state gas flux through the film (cm<sup>3</sup> (STP)/(cm<sup>2</sup> s)),  $l$  is the film thickness (cm), and  $f_{2,A}$  and  $f_{1,A}$  are the upstream and downstream fugacities of A (cmHg), respectively. Permeability coefficients are often expressed in units of barrer, where 1 barrer = 1 × 10<sup>-10</sup> (cm<sup>3</sup> (STP) · cm / cm<sup>2</sup> · s · cmHg).

The fugacity of gas A is calculated as follows [31]:

$$f_A = \phi_A x_A p \quad (2)$$

where  $\phi_A$  is the fugacity coefficient of A,  $x_A$  is the mole fraction of A, and  $p$  is the total pressure (atm). The information used to calculate the fugacity coefficients is provided elsewhere [32]. It is reasonable to replace  $f_{2,A}$  and  $f_{1,A}$  by  $p_{2,A}$  and  $p_{1,A}$  (*i.e.*, the upstream and downstream partial pressures of A (cmHg), respectively) in Eq. (1) to calculate pure gas permeabilities, because all gases and vapors exhibit nearly ideal behavior at the temperatures and pressures considered in this study. To calculate mixed gas permeabilities, fugacity is used instead of partial pressure because the *n*-C<sub>4</sub>H<sub>10</sub>/CH<sub>4</sub> mixtures at 35 °C exhibit non-ideal gas behavior, particularly at some of the higher values of feed pressure considered [33].

For dense polymeric membranes, the solution-diffusion model [34] describes the transport of gas molecules in polymers. In this model, gas dissolves on the feed side of the film, then diffuses through the film, and desorbs from the permeate side of the film. If the diffusion process is Fickian and the downstream (*i.e.*, permeate) pressure is far less than the upstream (*i.e.*, feed) pressure, then the permeability can be expressed as [35]:

$$P_A = D_A \times S_A \quad (3)$$

where  $D_A$  is the average effective diffusivity (cm<sup>2</sup>/s), and  $S_A$  is the apparent sorption (or solubility) coefficient of gas A in the polymer (cm<sup>3</sup> (STP)/(cm<sup>3</sup> polymer cmHg)). The solubility coefficient of A is defined as follows [36]:

$$S_A = C_{2,A} / f_{2,A} \quad (4)$$

where  $C_{2,A}$  is the gas concentration sorbed in the polymer at the upstream face of the film (cm<sup>3</sup> (STP)/cm<sup>3</sup> polymer), and  $f_{2,A}$  is the upstream fugacity of A (cmHg). For the pure gas sorption experiments considered in this study, the fugacity in Eq. (4) can be adequately approximated by  $p_{2,A}$ , the upstream pressure of A.

The ideal selectivity of a membrane for gas A over gas B is the ratio of their pure gas permeabilities; the most permeable gas is usually in the numerator of the following expression [35]:

$$\alpha_{A/B} = \frac{P_A}{P_B} = \left[ \frac{D_A}{D_B} \right] \times \left[ \frac{S_A}{S_B} \right] \quad (5)$$

where  $D_A/D_B$  is the diffusivity selectivity, which is the ratio of the diffusion coefficients of gases A and B. Larger gas molecules generally have smaller diffusion coefficients than smaller molecules. The ratio of solubility coefficients of gases A and B,  $S_A/S_B$ , is the solubility selectivity. The term “reverse-selectivity” refers to polymers being more permeable to larger, more soluble molecules, such as *n*-C<sub>4</sub>H<sub>10</sub>, than to smaller, less soluble gases such as CH<sub>4</sub>. This phenomenon can occur when  $D_A/D_B$ , the diffusivity selectivity, approaches unity and the solubility selectivity,  $S_A/S_B$ , is significantly larger than 1 [29,30,35].

Diffusion of small molecules in dense polymeric films is also understood to be a function of polymer free volume, and the following model is often used to describe this dependence [37]:

$$D_A = C \exp\left(-\frac{\gamma}{\langle V_f \rangle} V_A^*\right) \quad (6)$$

where  $C$  is a pre-exponential factor,  $\gamma$  is a numerical factor introduced to account for overlap of free volume,  $V_A^*$  is the minimum free volume element size needed to accommodate a gas molecule, and  $\langle V_f \rangle$  is the average free volume in the polymer. In this model, the diffusion coefficient is a function of penetrant size and polymer average free volume. As average free volume increases, the effect of penetrant size on diffusivity diminishes, so the polymer becomes less size-sieving. This trend is especially true for high free volume PTMSP, and it is an important consideration for understanding the transport properties of reverse-selective separation materials.

$\langle V_f \rangle$  is usually replaced by fractional free volume (FFV) in gas diffusion studies. A group contribution method is used to calculate FFV [38–40]. The van der Waals volume of each molecular group in the polymer is summed and multiplied by 1.3 to find the total occupied volume of the polymer [38–40]. The FFV is related to the occupied volume and the polymer specific volume as follows [39]:

$$\text{FFV} = \frac{V - V_o}{V} \quad (7)$$

where  $V$  is the specific volume of the polymer film ( $\text{cm}^3/\text{g}$ ), and  $V_o$  is the occupied volume ( $\text{cm}^3/\text{g}$ ).

Because solubility is typically a weak function of free volume, permeability often exhibits a similar dependence on free volume as diffusivity [37]:

$$P_A = S_A C \exp\left(-\frac{\gamma}{\langle V_f \rangle} V_A^*\right) \quad (8)$$

## 2. Experimental

### 2.1. Materials

Ultra high purity (99.99%) cylinders of  $\text{N}_2$  and  $\text{O}_2$ , and chemical purity (99%) cylinders of  $\text{CH}_4$ ,  $\text{C}_2\text{H}_6$ ,  $\text{C}_3\text{H}_8$ , and  $n\text{-C}_4\text{H}_{10}$  were received from Air Gas Southwest Inc. (Corpus Christi, TX). Mixtures of  $\text{CH}_4$  and  $n\text{-C}_4\text{H}_{10}$  were received from Air Liquide America Corporation (Houston, TX). All gases were used as-received. Poly(1-trimethylsilyl-1-propyne) (PTMSP) was kindly supplied by Air Products and Chemicals, Inc. The bis(azide) crosslinkers initially chosen to crosslink PTMSP were: 3,3'-diazidodiphenylsulfone, 2,6-di(*p*-azidobenzyl)-4-methylcyclohexanone, and 2,6-bis(4-azidobenzylidene)cyclohexanone. All were supplied by Sigma Aldrich Chemicals. These bis(azide)s were chosen because they are chemically safe at the conditions of film formation and crosslinking, have been shown to crosslink polymeric materials

effectively, and are commercially available at a reasonable price [41–45]. Nonporous, hydrophobic fumed silica nanoparticles (FS) (Cab-O-Sil TS530, a grade of FS available from Cabot Corp., Tuscola, IL) were added to PTMSP to form nanocomposite films. TS530 FS nanoparticles have a characteristic dimension of 13 nm, and they have been chemically treated with hexamethyldisilazane to replace hydrophilic hydroxyl surface groups with hydrophobic trimethylsilyl surface groups [46]. TEM imaging of nanocomposite films of PTMSP and fumed silica by De Sitter et al. showed that the silica particles were aggregated in the polymer matrixes in the size range of several hundred nanometers [47]. Merkel et al. showed that mean fumed silica aggregate size in poly-(4-methyl-2-pentyne) [PMP] nanocomposite films was in the range of 70–110 nm [48]. The nanocomposite films in this study were prepared using a similar physical dispersion/solution casting method as used by De Sitter et al. and Merkel et al., so it is reasonable to expect FS agglomerates in our films to be in this size range. All solvents used in the experiments had a purity of at least 99.8%. All materials and chemicals were used as-received unless otherwise indicated.

### 2.2. Film preparation

Dense films of PTMSP and bis(azide) crosslinker (XL) were cast from a toluene solution containing 1.5 wt.% polymer. FS nanoparticles were added to these solutions if the final films were going to be nanocomposite films. The solutions were stirred for 2 days using a magnetic stir bar, and the cast films were dried at ambient conditions for approximately 1 week until all toluene had evaporated. A variety of commercially available bis(azide)s were considered for these studies. However, the most effective crosslinker for PTMSP was 3,3'-diazidodiphenylsulfone. Its chemical structure is shown in Fig. 1. This crosslinker was chosen because films crosslinked with 3,3'-diazidodiphenylsulfone were less soluble in toluene (a good solvent for PTMSP [2]) than films crosslinked with equivalent amounts of other bis(azide)s considered, such as 2,6-di(*p*-azidobenzyl)-4-methylcyclohexanone or 2,6-bis(4-azidobenzylidene)cyclohexanone. A possible reason for this behavior is that 2,6-di(*p*-azidobenzyl)-4-methylcyclohexanone and 2,6-bis(4-azidobenzylidene)cyclohexanone contain 30 wt.% water (to allow safe handling of them); since PTMSP has a low affinity for water, the water content makes the bis(azide)s less compatible with PTMSP [49].

All films containing 3,3'-diazidodiphenylsulfone crosslinker were crosslinked in a vacuum oven at 180 °C for 90 min. The decision to thermally crosslink PTMSP was chosen because Jia and Baker found a smaller decrease in

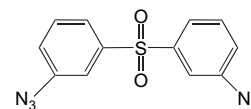


Fig. 1. Chemical structure of bis(azide) crosslinker 3,3'-diazidodiphenylsulfone.

permeability when films were crosslinked thermally than when crosslinking was initiated by *uv* light [25]. The crosslinking reaction was performed in the absence of oxygen because nitrene molecules oxidize to form nitroso compounds, which reduces the effectiveness of the crosslinking reaction [45]. A temperature of 180 °C was required to facilitate formation of a bis(nitrene) from its respective bis(azide) crosslinker; at lower temperatures, the reaction did not proceed at a reasonable rate. After 90 min in the vacuum oven, the peak associated with the azide group in the FT-IR spectrum at 2120 cm<sup>-1</sup> disappeared, indicating that the azide molecules had reacted to form nitrenes.

PTMSP displays strong hysteresis effects with respect to its transport properties, FFV, and positron annihilation lifetime spectroscopy parameters [14,15,18,50,51]. To insure preparation of PTMSP samples with reproducible properties, all films were soaked in methanol (MeOH), which is a swelling non-solvent for PTMSP, for 24 h following film preparation and exposure to high temperature under vacuum to bring about crosslinking. The length of the MeOH immersion insures MeOH reaches equilibrium with the PTMSP films [18]. This step helps to minimize sample to sample variability due to slight differences in thermal processing history [18]. PTMSP permeation properties are sensitive to thermal history [15], so care is required when preparing and crosslinking PTMSP. Crosslinking time and temperature are kept constant so that each sample has the same thermal history. It is important to insure that no contaminants (*e.g.*, vacuum pump oil vapors) contact the film during film preparation and crosslinking [2], because these materials can alter the transport properties. Contamination by vacuum pump oil vapors was minimized by using two liquid N<sub>2</sub> traps on the line between the vacuum pump and the vacuum oven. The films were dried at ambient conditions for 72 h after soaking to ensure that all MeOH has evaporated from the films [18]. Afterwards, film thickness was measured, and transport property testing was commenced. Films used in pure gas permeation and sorption experiments were approximately 100 μm thick, and films used in mixed gas permeation experiments were approximately 500 μm thick.

### 2.3. Permeation measurements

#### 2.3.1. Pure gas

Pure gas permeabilities were determined in a constant pressure, variable volume permeation cell. At steady state, the following expression was used to evaluate the permeability of gas A in a film [35]:

$$P_A = \frac{1}{A} \times \frac{V}{t} \times \frac{l}{p_2 - p_1} \times \frac{273.15K}{T} \times \frac{p_a}{76} \times 10^{10} \quad (9)$$

where  $P_A$  is the permeability coefficient (barrer),  $A$  is the film area (cm<sup>2</sup>),  $V$  is the steady state volume of permeating gas (cm<sup>3</sup>) collected during a time,  $t$ (s),  $l$  is film thickness (cm),  $p_2$  is gas pressure of A on the upstream (*i.e.*, high pressure) side of the film (cmHg),  $p_1$  is the gas pressure on the downstream (*i.e.*, low pressure) side of the film (cmHg),  $T$  is the

measurement temperature (K), and  $p_a$  is atmospheric pressure (cmHg). The area of the films was 13.8 cm<sup>2</sup>, and gas flow rates were measured using a bubble flow meter. The gases were tested in the following order: N<sub>2</sub>, O<sub>2</sub>, CH<sub>4</sub>, C<sub>2</sub>H<sub>6</sub>, C<sub>3</sub>H<sub>8</sub>, and *n*-C<sub>4</sub>H<sub>10</sub>. N<sub>2</sub> permeability was measured before and after each gas to check for any conditioning effects that the previous permeating gas may have had on the PTMSP films. Permeation measurements with permanent gases (N<sub>2</sub>, O<sub>2</sub>, CH<sub>4</sub>, C<sub>2</sub>H<sub>6</sub>) were performed at 35 °C and an upstream pressure of 4.4 atm. The permeability coefficients of C<sub>3</sub>H<sub>8</sub> and *n*-C<sub>4</sub>H<sub>10</sub> were measured at 35 °C and upstream pressures of 2.8 atm and 1.3 atm, respectively. The downstream pressure in all cases was atmospheric.

#### 2.3.2. Mixed gas

Mixed gas permeabilities were measured using a constant pressure, variable volume system connected to a gas chromatograph equipped with a thermal conductivity detector (TCD) and a flame ionization detector (FID) [4]. By measuring the permeate concentration of gas A in the sweep,  $x_{1A}$ , and the sweep gas flow rate,  $S$  (cm<sup>3</sup>/s), the permeability of gas A was calculated as follows [4]:

$$P_A = \frac{x_{1A} S l}{x_c^p A (f_{2,A} - f_{1,A})} \times \frac{273.15K}{T} \times \frac{p_a}{76} \times 10^{10} \quad (10)$$

where  $f_{2,A}$  and  $f_{1,A}$  are the feed and permeate fugacities of gas A, and  $x_c^p$  is the mole fraction of sweep gas in the permeate stream. The ratio of permeate to feed flow rate (*i.e.*, stage cut), was always less than 1%. Under these conditions, the residue and feed compositions were essentially equal. Helium was used as the sweep gas in this study. The mixed gas permeation films are thicker than the pure gas permeation films so that the flux of gas permeating across the film is reduced in the mixed gas experiments. In this way, a lower flow rate of residue gas is required to maintain the stage cut below 1%, which minimizes the consumption of feed gas. Mixed gas selectivity values were calculated as the ratio of the permeability coefficients determined in the mixed gas permeation experiment, as indicated in Eq. (5).

### 2.4. Sorption measurements

Sorption isotherms in uncrosslinked and crosslinked PTMSP were determined in a high-pressure barometric sorption apparatus [52]. The apparatus consists of a charge cell and a sample cell, and the volumes of each cell are known. The cells were kept at constant temperature in a water bath. A known volume of polymer was placed in the sample cell, and both the charge and sample cells were exposed to vacuum overnight to degas the sample. The valve between the cells was then closed, penetrant gas was introduced into the charge cell and allowed to equilibrate, and the pressure was measured. The valve between the charge and sample cells was opened, introducing penetrant gas into the sample cell. The system was allowed to equilibrate, and the pressure was measured in both cells. Once both cell pressures had equilibrated, the



process was repeated, and penetrant uptake was measured as a function of pressure. The time required to reach equilibrium was, at most, a few hours. After measuring each sorption isotherm, the polymer samples were degassed overnight before the next isotherm was measured.

### 3. Results and discussion

#### 3.1. Crosslinking PTMSP

Crosslinking renders PTMSP insoluble in solvents that readily dissolve the uncrosslinked polymer [24–26]. Therefore, a preliminary indication of successful crosslinking is the lack of solubility of crosslinked films in known solvents for PTMSP. In this study, crosslinked PTMSP was insoluble in toluene, cyclohexane and tetrahydrofuran (THF), which are excellent solvents for uncrosslinked PTMSP [1]. For example, as shown in Table 1, when the crosslinker concentration is 2.4 wt.% or greater, PTMSP films are insoluble in toluene. Insolubility of crosslinked PTMSP films is defined when there is less than 1% weight loss in a dry film before and after soaking in toluene for 24 h. Crosslinked PTMSP films have been soaked in toluene for up to 2 years and, even after this long exposure period, the films remained insoluble.

The theoretical number of monomers between each crosslink is estimated using the following expression [53]:

$$N_m = \frac{W_P/M_P}{W_{XL}/(2M_{XL})} \quad (11)$$

where  $N_m$  is the average number of monomer units between crosslinks,  $W_P$  is the mass of PTMSP in the film (g),  $M_P$  is the molecular weight of the PTMSP repeat unit (g/mol),  $W_{XL}$  is the mass of bis(azide) in the film (g), and  $M_{XL}$  (g/mol) is the bis(azide) molecular weight (300 g/mol). This calculation assumes that every azide moiety reacts and abstracts one hydrogen from a PTMSP repeat unit.

A plausible mechanism for the crosslinking reaction is presented in Fig. 2 [24,25]. After azide decomposition, the resulting nitrenes insert into a carbon–hydrogen bond in PTMSP to form a substituted amine. Since allylic C–H bonds are significantly weaker ( $\sim 85$  kcal/mol) [54] than the C–H bonds in  $\text{Si}(\text{CH}_3)_3$  ( $\sim 100$  kcal/mol) [54], reaction at the allylic methyl groups ( $\text{C}=\text{C}-\text{CH}_3$ ) along the PTMSP backbone should be strongly favored [55]. Further support for this mechanism was obtained by examining FT-IR spectra of the crosslinked films which is shown in Fig. 3. The intensity of the characteristic signals attributed to the alkene units in PTMSP ( $1600\text{ cm}^{-1}$ ,

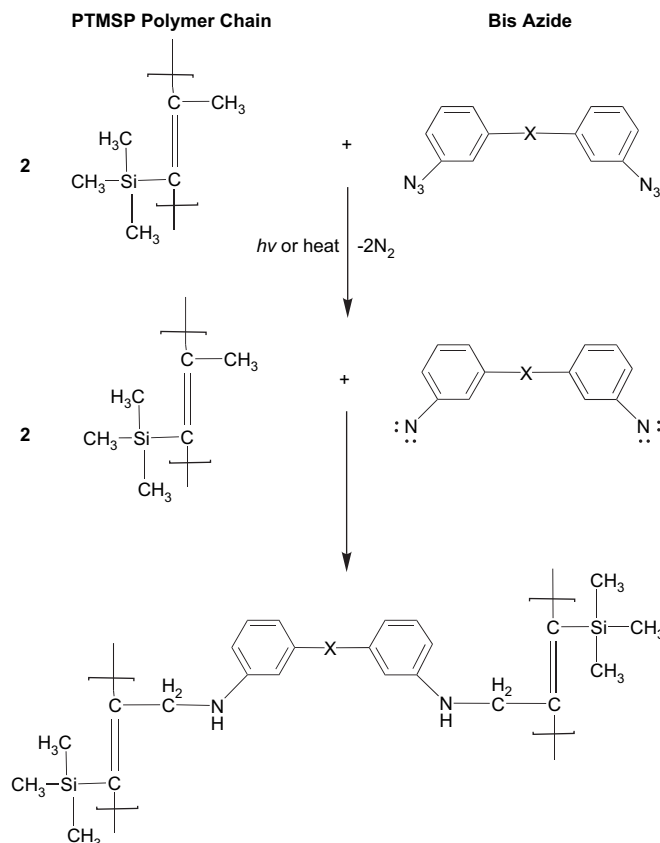


Fig. 2. Proposed reaction scheme for crosslinking PTMSP with bis(azide)s [24].

$\text{C}=\text{C}$  stretching) did not decrease upon crosslinking. This result effectively minimizes the possibility of a nitrene addition-type mechanism, which would connect polymer chains via an aziridine linkage. The azide peak at  $2120\text{ cm}^{-1}$  disappears when the PTMSP film is crosslinked, indicating conversion of the bis(azide) crosslinker to a reactive bis(nitrene).

#### 3.2. Pure gas permeability

For all gases considered, permeability decreases as crosslinker content increases, and density decreases, which reduces free volume. Fig. 4 presents a typical example of such results.  $\text{N}_2$  permeability decreases from 7400 barrers to 2000 barrers as crosslinker content increases from 0 to 20 wt.%, while FFV decreases from 0.294 to 0.24. The FFV values of crosslinked samples are calculated using measured density values and Bondi's group contribution method [38–40].

Table 1  
Solubility of crosslinked PTMSP films in toluene

Crosslinker (wt.%)	0	0.7	1.4	2.4	4.9	7.7	10	20
Toluene soluble <sup>a</sup>	Yes	Yes	Partially	No	No	No	No	No
Monomer units between crosslinks <sup>b</sup>	–	–	90	55	26	16	12	6

<sup>a</sup> Films were soaked in toluene for 24 h. The films mass was measured before and after toluene immersion once all of the toluene had evaporated from the sample.

<sup>b</sup> Calculated according to Eq. (11).

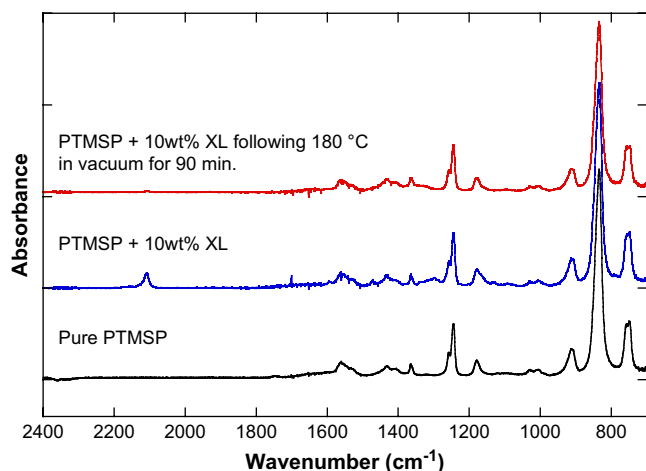


Fig. 3. FT-IR spectra of pure PTMSP, PTMSP containing 10 wt.% crosslinker (XL) prior to exposing the sample to elevated temperature to perform the crosslinking reaction, and crosslinked PTMSP containing 10 wt.% crosslinker.

It is of interest to understand whether the decrease in FFV associated with higher crosslinker content is due to the presence of the crosslinker in PTMSP or related to densification induced by the thermal annealing protocol. In this regard, the FFV of a PTMSP film containing 5 wt.% crosslinker is the same before and after exposure to the crosslinking conditions (180 °C for 90 min in vacuum). Therefore, the reduction in free volume is due to the mixing of high free volume PTMSP with the initially crystalline crosslinker, which is expected to have a much lower inherent FFV than PTMSP, rather than to thermally induced densification of the polymer.

The decrease in permeability can be correlated with the decrease in FFV [23]. The relationship between gas permeability

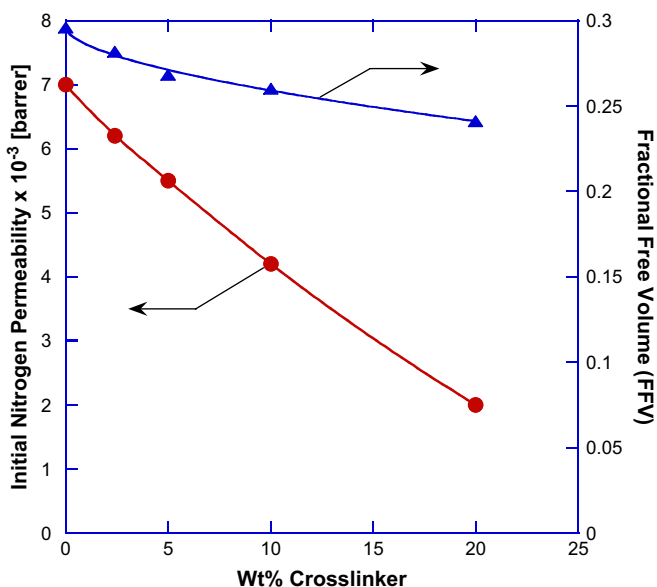


Fig. 4. Effect of crosslinker content on initial  $N_2$  permeability and FFV of PTMSP and crosslinked PTMSP films.  $T = 35$  °C,  $p_2 = 4.4$  atm, and  $p_1 =$  atmospheric for all measurements. All films were crosslinked in vacuum at 180 °C for 90 min, then soaked in MeOH for 24 h, and finally dried at ambient conditions for 72 h prior to the permeation measurements. Film thickness was approximately 100  $\mu$ m.

and FFV is presented in Fig. 5. The  $N_2$  permeability decreases from 7000 barrers to 4200 barrers, and the  $n\text{-}C_4H_{10}$  permeability decreases from 52,000 barrers to 40,000 barrers as the bis-(azide) content increases from 0 to 10 wt.%. The gas and vapor permeabilities for uncrosslinked PTMSP are consistent with values at the same pressures and temperatures reported by Merkel et al. [56]. A strong relationship between permeability and  $1/\text{FFV}$  is observed for all gases considered, which is consistent with Eq. (8) [23]. An increase in the  $O_2/N_2$  selectivity from 1.37 to 1.5 is observed as crosslinker content increases from 0 to 10 wt.%, suggesting a slight increase in size selectivity upon crosslinking. These results are consistent with the tradeoff between permeability and selectivity commonly observed in polymers [57,58].

### 3.3. Solubility and diffusivity

The permeability in a dense polymer is a function of gas diffusivity and gas solubility. Fig. 6(a–f) presents sorption isotherms of  $N_2$ ,  $O_2$ ,  $CH_4$ ,  $C_2H_6$ ,  $C_3H_8$ , and  $n\text{-}C_4H_{10}$  in uncrosslinked and crosslinked PTMSP at 35 °C. Within the uncertainty of this measurement, the sorption of  $N_2$ ,  $O_2$ ,  $CH_4$ ,  $C_2H_6$ ,  $C_3H_8$ , and  $n\text{-}C_4H_{10}$  in crosslinked PTMSP is the same as in uncrosslinked PTMSP. Therefore, gas and vapor solubility coefficients in PTMSP are not measurably affected by the FFV decrease accompanying crosslinking. The sorption data for a PTMSP film that was not crosslinked and not exposed to high temperatures were fit to the dual mode sorption equation [35], and a good fit was found for all gases and

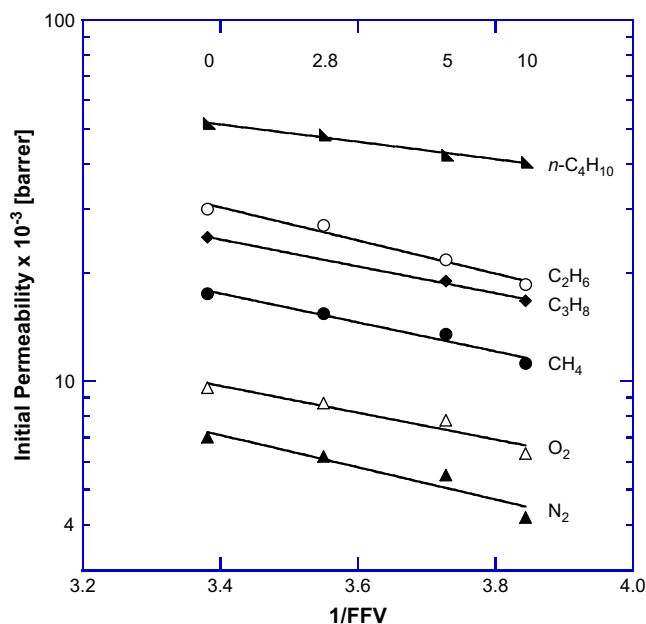


Fig. 5. Permeability of  $N_2$ ,  $O_2$ ,  $CH_4$ ,  $C_2H_6$ ,  $C_3H_8$  and  $n\text{-}C_4H_{10}$  in uncrosslinked and crosslinked PTMSP versus  $1/\text{FFV}$ .  $T = 35$  °C,  $p_2 = 4.4$  atm ( $N_2$ ,  $O_2$ ,  $CH_4$ , and  $C_2H_6$ ),  $p_2 = 2.8$  atm ( $C_3H_8$ ) and  $p_2 = 1.3$  atm ( $n\text{-}C_4H_{10}$ ),  $p_2 =$  atmospheric for all measurements. Films were crosslinked at 180 °C in vacuum for 90 min and soaked in MeOH for 24 h, then dried for 72 h before testing began. Film thickness was approximately 100  $\mu$ m. The numbers at the top of the plot represent the wt.% crosslinker initially present in the film.

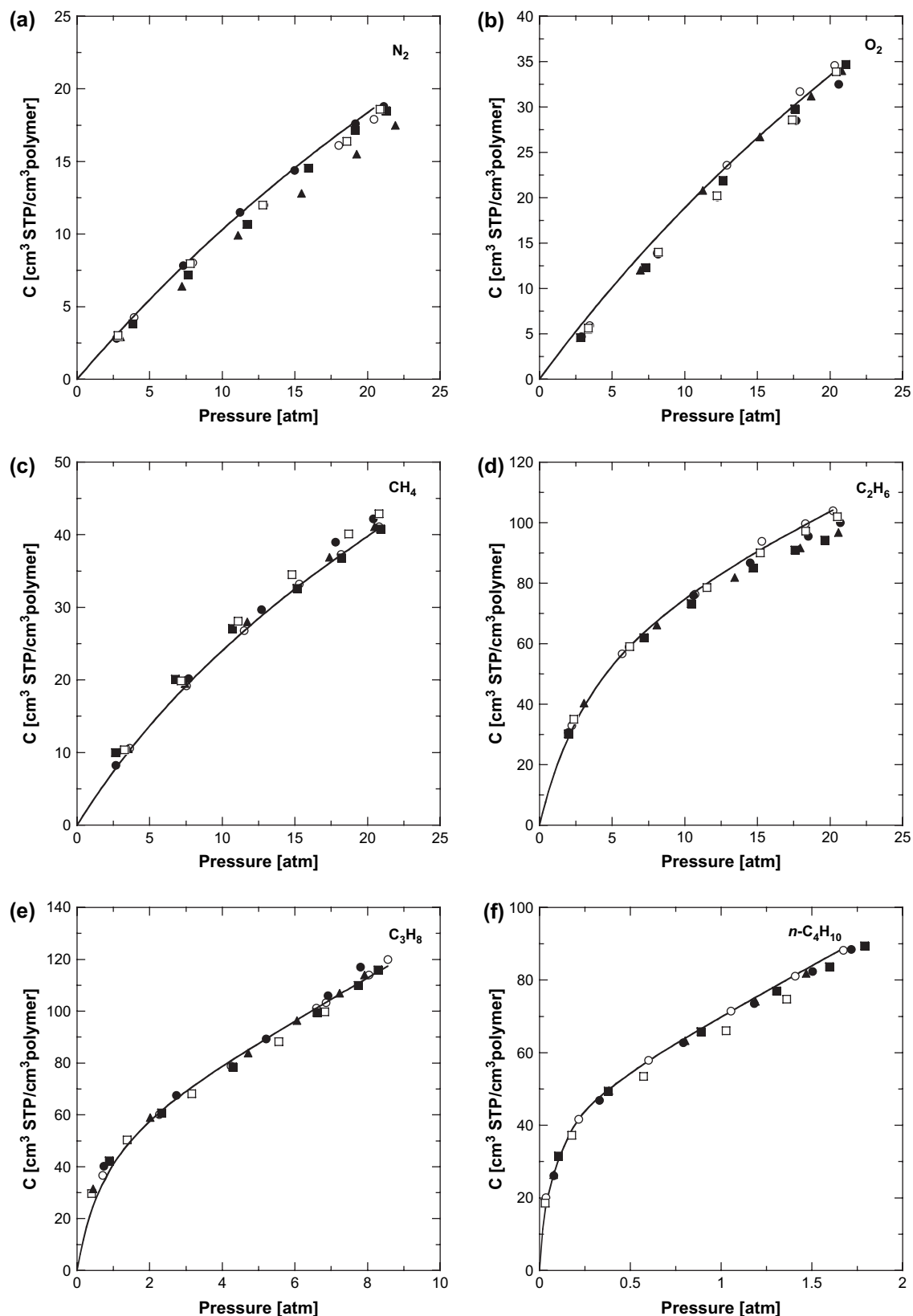


Fig. 6. Sorption isotherms of uncrosslinked and crosslinked PTMSP at 35 °C. (a) N<sub>2</sub>; (b) O<sub>2</sub>; (c) CH<sub>4</sub>; (d) C<sub>2</sub>H<sub>6</sub>; (e) C<sub>3</sub>H<sub>8</sub>; (f) n-C<sub>4</sub>H<sub>10</sub>. Except for the untreated PTMSP film, all films were crosslinked at 180 °C in vacuum for 90 min. All films were soaked in MeOH for 24 h and dried at ambient conditions for 72 h before measurements began. The line of best fit in each figure was found by fitting the dual mode sorption isotherm [35] to the uncrosslinked film that had not been subjected to thermal annealing. The symbols represent the following films: ○ – PTMSP untreated (*i.e.*, sample not exposed to 180 °C and no crosslinker), ● – PTMSP treated (*i.e.*, sample without crosslinker exposed to 180 °C in vacuum for 90 min), ▲ – PTMSP + 2.8 wt.% XL, ■ – PTMSP + 5 wt.% XL, and □ – PTMSP + 10 wt.% XL.

Table 2  
Comparison of pure gas dual mode model parameters for uncrosslinked PTMSP at 308 K

Gas	$k_D$ (cm <sup>3</sup> (STP)/cm <sup>3</sup> atm)	$b$ (atm <sup>-1</sup> )	$C'_H$ (cm <sup>3</sup> (STP)/cm <sup>3</sup> )	Reference
N <sub>2</sub>	0.08 ± 0.02	0.015 ± 0.001	70 ± 3	This work
	0.08	0.014	74	Merkel et al. [56]
O <sub>2</sub>	0.31 ± 0.07	0.019 ± 0.001	99 ± 4	This work
	0.19	0.014	80	Merkel et al.
CH <sub>4</sub>	0.74 ± 0.07	0.050 ± 0.004	50 ± 3	This work
	0.50	0.05	62	Merkel et al.
C <sub>2</sub> H <sub>6</sub>	2.0 ± 0.2	0.26 ± 0.03	76 ± 3	This work
	1.3	0.31	71	Merkel et al.
C <sub>3</sub> H <sub>8</sub>	7.7 ± 0.3	1.7 ± 0.3	55 ± 2	This work
	5.3	1.1	60	Merkel et al.
	5.8	2.5	50	Morisato et al.
<i>n</i> -C <sub>4</sub> H <sub>10</sub>	27 ± 2	21 ± 4	45 ± 2	This work
	27.7	14.8	44	Morisato et al. [59]

vapors. The dual mode model parameters for PTMSP from this study are shown in Table 2, and they are similar to the dual mode model parameters found by Merkel et al. [56], and Morisato et al. [59].

Because gas solubility is not measurably influenced by crosslinking, the decrease in gas permeability in crosslinked PTMSP is due mainly to a decrease in gas diffusivity. The gas diffusivities are calculated according to Eq. (3), using the measured gas permeabilities and solubilities. Fig. 7

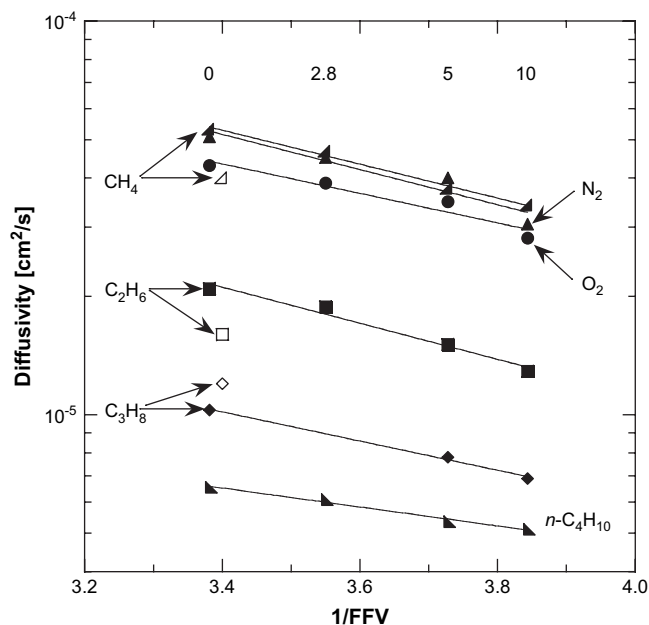


Fig. 7. Diffusivity of N<sub>2</sub>, O<sub>2</sub>, CH<sub>4</sub>, C<sub>2</sub>H<sub>6</sub>, C<sub>3</sub>H<sub>8</sub> and *n*-C<sub>4</sub>H<sub>10</sub> in uncrosslinked and crosslinked PTMSP versus 1/FFV at 35 °C. The diffusivity values were calculated at  $p_2 = 4.4$  atm (N<sub>2</sub>, O<sub>2</sub>, CH<sub>4</sub>, and C<sub>2</sub>H<sub>6</sub>),  $p_2 = 2.8$  atm (C<sub>3</sub>H<sub>8</sub>) and  $p_2 = 1.3$  atm (*n*-C<sub>4</sub>H<sub>10</sub>),  $p_1 =$  ambient in all cases. The filled symbols represent data from this study, while the open symbols represent data from Merkel et al. for uncrosslinked PTMSP at the same pressure and temperature [56]. Films were crosslinked at 180 °C in vacuum for 90 min and soaked in MeOH for 24 h, then dried for 72 h before permeation and sorption measurements began. Film thickness was approximately 100 μm. The numbers at the top of the plot represent the wt.% of crosslinker initially present in the film.

presents the relationship between gas diffusivity in uncrosslinked and crosslinked PTMSP and 1/FFV. The diffusivities decrease as FFV decreases and as crosslinker content increases. This result is expected according to Eq. (5), since diffusivity is a strong function of FFV [37]. In Fig. 7, the diffusivities of uncrosslinked PTMSP sample are compared to the CH<sub>4</sub>, C<sub>2</sub>H<sub>6</sub>, and C<sub>3</sub>H<sub>8</sub> diffusivities of uncrosslinked PTMSP reported by Merkel et al. [56] at the same pressure and temperature. The values from this study are similar to the literature values. The N<sub>2</sub>, O<sub>2</sub> and CH<sub>4</sub> diffusion coefficients are an order of magnitude greater than the C<sub>3</sub>H<sub>8</sub> and *n*-C<sub>4</sub>H<sub>10</sub> diffusion coefficients, since the kinetic diameters of C<sub>3</sub>H<sub>8</sub> and *n*-C<sub>4</sub>H<sub>10</sub> are at least 0.5 Å larger than those of N<sub>2</sub>, O<sub>2</sub> and CH<sub>4</sub> [60]. The same trend was found by Merkel et al. for uncrosslinked PTMSP [56].

### 3.4. Nanoparticle addition to crosslinked PTMSP

Adding nanosized, inorganic particles such as TS530 fumed silica (FS) to high free volume polymers can increase their permeability [61]. The permeability of filled glassy polymers is enhanced because the nanoparticles frustrate polymer chain packing. The nanoparticles increase free volume and, possibly, the connectivity of free volume elements, which increases permeability [10]. PTMSP films containing TS530 FS and bis(azide) crosslinkers were thermally crosslinked, and they were insoluble in common PTMSP solvents such as toluene. Fig. 8 illustrates the initial N<sub>2</sub> permeability of uncrosslinked and crosslinked PTMSP nanocomposite films containing 30 wt.% TS530 FS. In all cases, there is a substantial

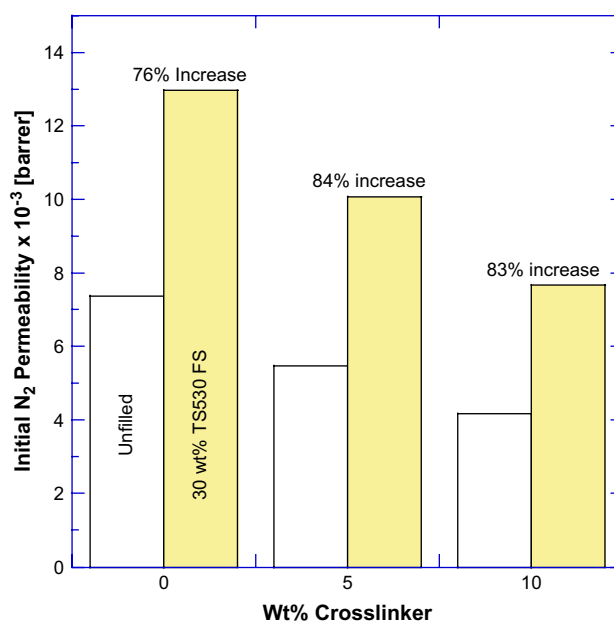


Fig. 8. N<sub>2</sub> permeability in uncrosslinked and crosslinked PTMSP films containing 0 and 30 wt.% TS530 FS.  $T = 35$  °C,  $p_2 = 4.4$  atm,  $p_1 =$  ambient. Films were crosslinked at 180 °C in vacuum for 90 min, soaked in MeOH for 24 h, and then dried for 72 h before testing began. Film thickness was approximately 100 μm. The percentage increase in permeability was calculated relative to the N<sub>2</sub> permeability of the films containing 0 wt.% TS530 FS.



increase in permeability due to nanoparticle addition, and the relative  $N_2$  permeability enhancement upon adding 30 wt.% TS530 FS is similar for all samples within the uncertainty of the experiment. At the same FS loadings, Merkel et al. and De Sitter et al. [47,48] observed a 62% and 75% increase in  $N_2$  permeability, respectively. These increases are similar to the approximately 80% permeability enhancement observed in our experiments, suggesting that the FS particle dispersion in our samples should be similar to the dispersion properties reported in the literature [47,48].

The effect of varying the FS content in crosslinked PTMSP films containing 10 wt.% crosslinker is presented in Fig. 9. As TS530 FS content increases from 0 to 15 wt.%, the  $N_2$  permeability increases from 4200 barrers to 5200 barrers; at 30 wt.% FS content, the  $N_2$  permeability increases to 7700 barrers, and at 45 wt.% FS, the  $N_2$  permeability is 11,000 barrers.

### 3.5. Mixed gas permeation

PTMSP exhibits enhanced vapor/gas selectivity in mixed gas permeation experiments [4,6–8,10,62]. Table 3 presents pure gas  $CH_4$  and  $n-C_4H_{10}$  permeabilities and pure gas  $n-C_4H_{10}/CH_4$  selectivities at 35 °C measured in the mixed gas permeation cell. These permeability values are slightly greater than the values measured in the pure gas permeation cell, and the reason for this discrepancy is most likely due to differences in the downstream penetrant partial pressure in the pure and mixed gas cells [4]. The downstream of the mixed gas cell is swept with helium, while the pure gas permeation cell is at atmospheric pressure downstream. As expected, the pure

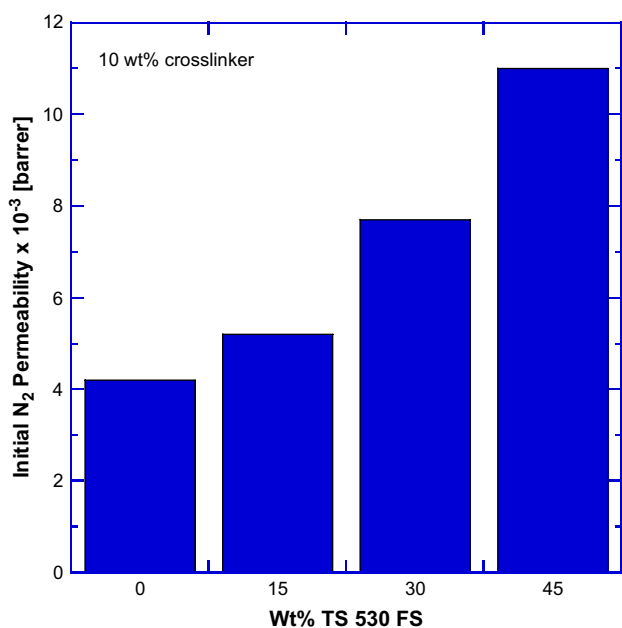


Fig. 9.  $N_2$  permeability in crosslinked PTMSP films containing various amounts of TS530 FS.  $T = 35$  °C,  $p_2 = 4.4$  atm,  $p_2 =$  ambient. Films were crosslinked at 180 °C in vacuum for 90 min, soaked in MeOH for 24 h, and then dried for 72 h before testing began. Film thickness was approximately 100  $\mu$ m.

Table 3

Pure gas  $n-C_4H_{10}$  and  $CH_4$  permeabilities and  $n-C_4H_{10}/CH_4$  selectivities at 35 °C measured in the mixed gas permeation cell

	Uncrosslinked PTMSP	Crosslinked PTMSP	Crosslinked PTMSP + 30 wt.% FS
$n-C_4H_{10}$ permeability (barrers)	70,000	58,000	80,000
$CH_4$ permeability (barrers)	20,000	15,000	24,000
$n-C_4H_{10}/CH_4$ selectivity	3.5	3.9	3.3

The crosslinked films contain 5 wt.% crosslinker. To ensure that the films experienced the same thermal history prior to permeation testing, all films were exposed to vacuum for 90 min at 180 °C, soaked in MeOH for 24 h, and dried for 72 h at ambient conditions before permeation testing began.  $CH_4$  permeabilities are reported at  $p_2 = 4.4$  atm, and  $n-C_4H_{10}$  permeabilities are reported at  $p_2 = 1.3$  atm. The downstream side of the film was swept with helium, so the downstream partial pressures of  $CH_4$  and  $n-C_4H_{10}$  were approximately 0 atm.

gas permeabilities for uncrosslinked PTMSP are greater than those of crosslinked PTMSP, while the addition of FS nanoparticles to crosslinked PTMSP increases its permeability substantially. There is no significant difference between the pure gas  $n-C_4H_{10}/CH_4$  selectivities of uncrosslinked and crosslinked PTMSP. The addition of nanoparticles decreases the pure gas  $n-C_4H_{10}/CH_4$  selectivity of crosslinked PTMSP slightly, and this is caused by an increase in the  $CH_4$  permeability relative to the  $n-C_4H_{10}$  permeability [10].

A gas mixture containing 98 mol%  $CH_4$  and 2 mol%  $n-C_4H_{10}$  was permeated through uncrosslinked PTMSP, crosslinked PTMSP, and crosslinked PTMSP containing 30 wt.% FS at fugacities ranging from 4.3 to 14.5 atm. Fig. 10 presents

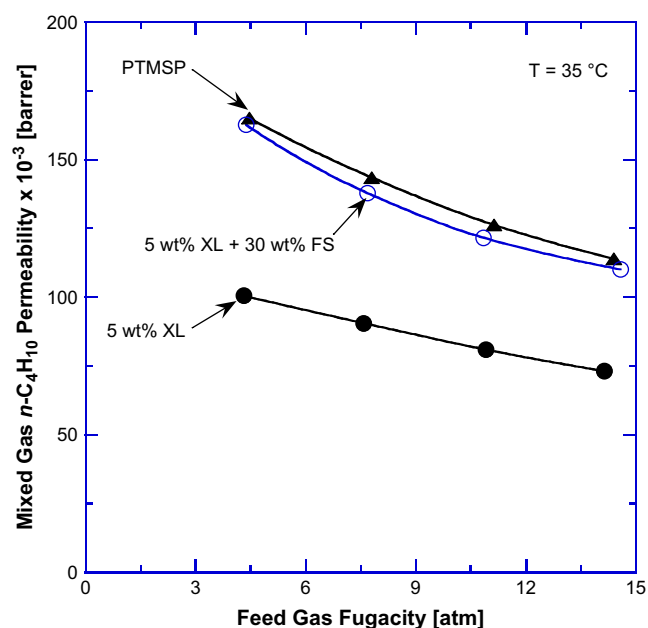


Fig. 10. Mixed gas  $n-C_4H_{10}$  permeability in uncrosslinked PTMSP and crosslinked PTMSP containing 5 wt.% crosslinker. The feed gas contained 98 mol%  $CH_4$  and 2 mol%  $n-C_4H_{10}$ , and the downstream side of the film was swept with helium. Films were crosslinked at 180 °C in vacuum for 3 h, soaked in MeOH for 24 h, and then dried for 72 h before testing began. Film thickness was approximately 500  $\mu$ m.

mixed gas  $n\text{-C}_4\text{H}_{10}$  permeability at 35 °C as a function of feed fugacity for uncrosslinked and crosslinked PTMSP films. The mixed gas  $n\text{-C}_4\text{H}_{10}$  permeabilities are lower in crosslinked PTMSP than in uncrosslinked PTMSP. This result is expected since the presence of the crosslinker decreases the polymer FFV. The addition of FS nanoparticles to crosslinked PTMSP increases the  $n\text{-C}_4\text{H}_{10}$  permeability, and this result is expected as FS addition has been shown to increase the free volume of PTMSP [10]. The  $n\text{-C}_4\text{H}_{10}$  permeability in all the films tested decreases as feed fugacity increases, and this effect is probably due to a decrease in  $n\text{-C}_4\text{H}_{10}$  solubility coefficient with increasing fugacity.

Fig. 11 presents the mixed gas  $\text{CH}_4$  permeability at 35 °C as a function of feed fugacity for uncrosslinked PTMSP, crosslinked PTMSP, and crosslinked PTMSP containing 30 wt.% FS. For all films tested, there is a substantial decrease in  $\text{CH}_4$  permeability as the feed gas fugacity and  $n\text{-C}_4\text{H}_{10}$  activity increases. The decrease in  $\text{CH}_4$  permeability is due to blocking [8]. Due to the very high FFV of PTMSP, there are numerous free volume elements that appear to be connected, forming something akin to a microporous network [3]. Most of the transport is believed to occur through this interconnected volume [3,8]. The condensable vapor (*i.e.*,  $n\text{-C}_4\text{H}_{10}$ ) sorbs into the free volume elements, thereby reducing the ability of less condensable gases, such as  $\text{CH}_4$ , to sorb and diffuse in these free volume elements. The blockage reduces the permeability of permanent gases (*e.g.*,  $\text{CH}_4$ ) [63,64]. In PTMSP, blocking has been observed for large, strongly sorbing organic vapors such as  $\text{C}_3\text{H}_8$  and  $n\text{-C}_4\text{H}_{10}$  [4,6–8,10,62] in mixtures with permanent gases such as  $\text{H}_2$  and  $\text{CH}_4$ . The addition of 30 wt.% FS to crosslinked PTMSP caused a greater relative

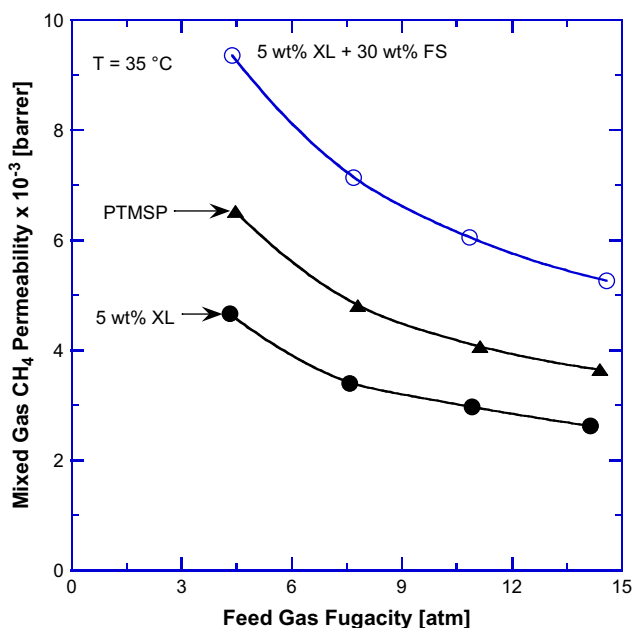


Fig. 11. Mixed gas  $\text{CH}_4$  permeability in uncrosslinked PTMSP and crosslinked PTMSP films. The feed gas contained 98 mol%  $\text{CH}_4$  and 2 mol%  $n\text{-C}_4\text{H}_{10}$ , and the downstream side of the film was swept with helium. Films were crosslinked at 180 °C in vacuum for 3 h, soaked in MeOH for 24 h, and then dried for 72 h before testing began. Film thickness was approximately 500  $\mu\text{m}$ .

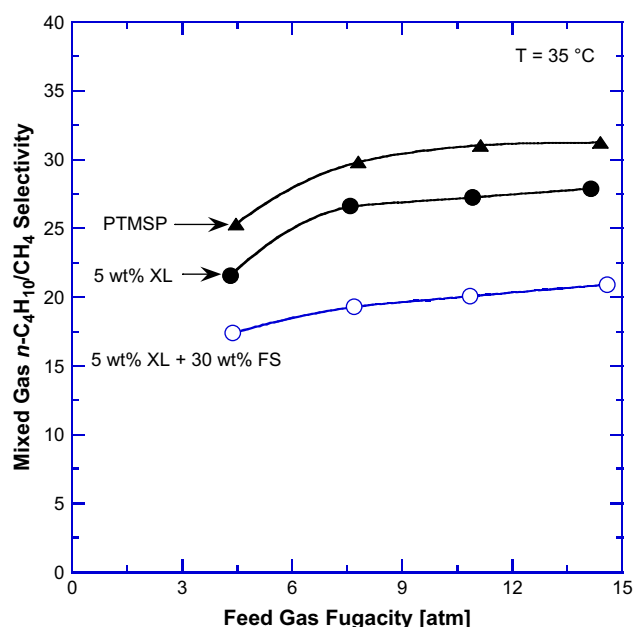


Fig. 12. Mixed gas  $n\text{-C}_4\text{H}_{10}/\text{CH}_4$  permeability in uncrosslinked PTMSP and crosslinked PTMSP films. The feed gas contained 98 mol%  $\text{CH}_4$  and 2 mol%  $n\text{-C}_4\text{H}_{10}$ , and the downstream side of the film was swept with helium. Films were crosslinked at 180 °C in vacuum for 3 h, soaked in MeOH for 24 h, and then dried for 72 h before testing began. Film thickness was approximately 500  $\mu\text{m}$ .

increase in the mixed gas  $\text{CH}_4$  permeability than in the mixed gas  $n\text{-C}_4\text{H}_{10}$  permeability. The mixed gas  $\text{CH}_4$  permeability of the crosslinked PTMSP containing 30 wt.% FS is substantially greater than that of uncrosslinked PTMSP, while the mixed gas  $n\text{-C}_4\text{H}_{10}$  permeabilities of these two films were similar. These results show that there is less blocking of the  $\text{CH}_4$  permeation by  $n\text{-C}_4\text{H}_{10}$  in the crosslinked PTMSP film containing 30 wt.% FS than in the uncrosslinked and crosslinked PTMSP films containing no FS nanoparticles. It was hypothesized by Merkel et al. [10] that the addition of FS to PTMSP creates free volume elements large enough to allow relatively non-selective transport mechanisms, such as Knudsen flow, to be important, and this hypothesis is consistent with our results.

Fig. 12 presents mixed gas  $n\text{-C}_4\text{H}_{10}/\text{CH}_4$  selectivities as a function of feed gas fugacity at 35 °C. For all films tested, the mixed gas  $n\text{-C}_4\text{H}_{10}/\text{CH}_4$  selectivity increases as feed gas fugacity increases due primarily to an increase in the blocking effect when  $n\text{-C}_4\text{H}_{10}$  activity in the feed increases. The  $n\text{-C}_4\text{H}_{10}/\text{CH}_4$  selectivities are slightly greater in uncrosslinked PTMSP films than in crosslinked films containing no FS nanoparticles. The crosslinked films have lower free volume and are slightly more size-sieving than their uncrosslinked analogs, which would be consistent with somewhat lower  $n\text{-C}_4\text{H}_{10}/\text{CH}_4$  mixture selectivity values in the crosslinked films. The addition of FS nanoparticles to crosslinked PTMSP decreases the  $n\text{-C}_4\text{H}_{10}/\text{CH}_4$  selectivities, and this decrease is caused by a decrease in the overall blocking effect in the nanocomposite film. The addition of FS nanoparticles creates large free volume elements, which are thought to make  $\text{CH}_4$

selective Knudsen flow more important in the overall transport mechanism [10], which decreases the mixed gas selectivity.

#### 4. Conclusion

PTMSP can be crosslinked using commercially available bis(azide)s. Crosslinking increases the solvent resistance of PTMSP, and crosslinked PTMSP is insoluble in good solvents for PTMSP, such as toluene. The permeability and FFV of crosslinked PTMSP decreased as crosslinker content increased, and permeability was found to be proportional to the exponential of  $1/FFV$ . Gas sorption properties were unaffected by crosslinking, while the diffusivity of crosslinked PTMSP decreased as crosslinker content increased. The diffusivity was proportional to the exponential of  $1/FFV$ , consistent with free volume theory. The addition of FS nanoparticles to crosslinked PTMSP caused the permeability to increase substantially. Like uncrosslinked PTMSP, crosslinked PTMSP displays high  $n\text{-C}_4\text{H}_{10}/\text{CH}_4$  selectivity, and blocking of  $\text{CH}_4$  permeation by more strongly sorbing  $n\text{-C}_4\text{H}_{10}$  molecules was observed. At 35 °C, the  $n\text{-C}_4\text{H}_{10}/\text{CH}_4$  selectivity in mixed gas experiments using crosslinked PTMSP was slightly lower than that of uncrosslinked PTMSP, while the addition of FS nanoparticles to crosslinked PTMSP further decreased the mixed gas  $n\text{-C}_4\text{H}_{10}/\text{CH}_4$  selectivity.

#### Acknowledgements

We gratefully acknowledge partial support of this work by the U.S. Department of Energy (DE-FG03-02ER15362) and the National Science Foundation (CBET-0515425).

#### References

- Masuda T, Isobe E, Higashimura T, Takada K. Poly[1-(trimethylsilyl)-1-propyne]: a new high polymer synthesized with transition-metal catalysts and characterized by extremely high gas permeability. *Journal of the American Chemical Society* 1983;105:7473–4.
- Nagai K, Masuda T, Nakagawa T, Freeman BD, Pinnau I. Poly[1-(trimethylsilyl)-1-propyne] and related polymers: synthesis, properties and functions. *Progress in Polymer Science* 2001;26:721–98.
- Srinivasan R, Auvil SR, Burban PM. Elucidating the mechanism(s) of gas transport in poly(1-(trimethylsilyl)-1-propyne) (PTMSP) membranes. *Journal of Membrane Science* 1994;86:67–86.
- Merkel TC, Gupta RP, Turk BS, Freeman BD. Mixed-gas permeation of syngas components in poly(dimethylsiloxane) and poly(1-(trimethylsilyl)-1-propyne) at elevated temperatures. *Journal of Membrane Science* 2001;191:85–94.
- Fried JR, Goyal DK. Molecular simulation of gas transport in poly[1-(trimethylsilyl)-1-propyne]. *Journal of Polymer Science Part B: Polymer Physics* 1998;36:519–36.
- Pinnau I, Casillas CG, Morisato A, Freeman BD. Hydrocarbon/hydrogen mixed gas permeation in poly(1-(trimethylsilyl)-1-propyne) (PTMSP), poly(1-phenyl-1-propyne) (PPP), and PTMSP/PPP blends. *Journal of Polymer Science Part B: Polymer Physics* 1996;34:2613–21.
- Pinnau I, Casillas CG, Morisato A, Freeman BD. Long-term permeation properties of poly(1-(trimethylsilyl)-1-propyne) membranes in hydrocarbon-vapor environment. *Journal of Polymer Science Part B: Polymer Physics* 1997;35:1483–90.
- Pinnau I, Toy LG. Transport of organic vapors through poly(1-(trimethylsilyl)-1-propyne). *Journal of Membrane Science* 1996;116:199–209.
- Teplyakov VV, Roizard D, Favre E, Khotimsky VS. Investigations on the peculiar permeation properties of volatile organic compounds and permanent gases through PTMSP. *Journal of Membrane Science* 2003;220:165–75.
- Merkel TC, He Z, Pinnau I, Freeman BD, Meakin P, Hill AJ. Effect of nanoparticles on gas sorption and transport in poly(1-(trimethylsilyl)-1-propyne). *Macromolecules* 2003;36:6844–55.
- Masuda T, Isobe E, Higashimura T. Polymerization of 1-(trimethylsilyl)-1-propyne by halides of niobium(V) and tantalum(V) and polymer properties. *Macromolecules* 1985;18:841–5.
- Dorkenoo KD, Pfromm PH. Accelerated physical aging of thin poly[1-(trimethylsilyl)-1-propyne] films. *Macromolecules* 2000;33:3747–51.
- Langsam M, Robeson LM. Substituted propyne polymers – part II. Effects of aging on the gas permeability properties of poly[1-(trimethylsilyl)propyne] for gas-separation membranes. *Polymer Engineering and Science* 1989;29:44–54.
- Nagai K, Freeman BD, Hill AJ. Effect of physical aging of poly(1-(trimethylsilyl)-1-propyne) films synthesized with  $\text{TaCl}_5$  and  $\text{NbCl}_5$  on gas permeability, fractional free volume, and positron annihilation lifetime spectroscopy parameters. *Journal of Polymer Science Part B: Polymer Physics* 2000;38:1222–39.
- Nagai K, Nakagawa T. Effects of aging on the gas permeability and solubility in poly(1-(trimethylsilyl)-1-propyne) membranes synthesized with various catalysts. *Journal of Membrane Science* 1995;105:261–72.
- Nakagawa T, Fujisaki S, Nakano H, Higuchi A. Physical modification of poly[1-(trimethylsilyl)-1-propyne] membranes for gas separation. *Journal of Membrane Science* 1994;94:183–93.
- Yampol'skii YP, Shishatskii SM, Shantorovich VP, Antipov EM, Kuzmain NN, Rykov SV, et al. Transport characteristics and other physicochemical properties of aged poly(1-(trimethylsilyl)-1-propyne). *Journal of Applied Polymer Science* 1993;48:1935–44.
- Hill AJ, Pas SJ, Bastow TJ, Burgar MI, Nagai K, Toy LG, et al. Influence of methanol conditioning and physical aging on carbon spin–lattice relaxation times of poly(1-(trimethylsilyl)-1-propyne). *Journal of Membrane Science* 2004;243:37–44.
- Baker RW. Future directions of membrane gas separation technology. *Industrial & Engineering Chemistry Research* 2002;41:1393–411.
- Bowmer TN, Baker GL. Thermal and radiolytic stability of halogenated derivatives of poly(trimethylsilyl propyne). *Polymer Preprints (American Chemical Society, Division of Polymer Chemistry)* 1986;27:218.
- Nagai K, Higuchi A, Nakagawa T. Gas permeation and sorption in brominated poly(1-(trimethylsilyl)-1-propyne) membrane. *Journal of Applied Polymer Science* 1994;54:1353–61.
- Nagai K, Mori M, Watanabe T, Nakagawa T. Gas permeation properties of blend and copolymer membranes composed of 1-(trimethylsilyl)-1-propyne and 1-phenyl-1-propyne structures. *Journal of Polymer Science Part B: Polymer Physics* 1997;35:119–31.
- Merkel TC, Toy LG, Andrady AL, Gracz H, Stejskal EO. Investigation of enhanced free volume in nanosilica-filled poly(1-(trimethylsilyl)-1-propyne) by  $^{129}\text{Xe}$  NMR spectroscopy. *Macromolecules* 2003;36:353–8.
- J. Jia, Gas separation and pervaporation of chemically modified poly(1-(trimethylsilyl)-1-propyne) membranes, Ph.D. dissertation, Michigan State University; 1999.
- Jia J, Baker GL. Crosslinking of poly[1-(trimethylsilyl)-1-propyne] membranes using bis(aryl azides). *Journal of Polymer Science Part B: Polymer Physics* 1998;36:959–68.
- Ruud CJ, Jia J, Baker GL. Synthesis and characterization of poly-[(1-(trimethylsilyl)-1-propyne)-co-(1-(4-azidobutyl)dimethylsilyl)-1-propyne)] copolymers. *Macromolecules* 2000;33:8184–91.
- Patai S. *The chemistry of the azido group*. 1st ed. London: John Wiley & Sons; 1971.
- Loudon GM. *Organic chemistry*. 3rd ed. Menlo Park, CA: Benjamin/Cummings Publishing Company; 1995. p. 1113–68.
- Freeman B, Pinnau I. Separation of gases using solubility-selective polymers. *Trends in Polymer Science* 1997;5:167–73 [Cambridge, United Kingdom].
- Matteucci S, Yampolskii Y, Freeman BD, Pinnau I. In: Yampolskii Y, Freeman BD, Pinnau I, editors. *Material science of membranes for gas and vapor separation*. New York: John Wiley & Sons; 2006. p. 1–47.

- [31] Smith JM, Van Ness HC, Abbot MM. Chemical engineering thermodynamics. 5th ed. New York: McGraw-Hill; 1995.
- [32] Lin H, Freeman BD. Gas and vapor solubility in cross-linked poly(ethylene glycol diacrylate). *Macromolecules* 2005;38:8394–407.
- [33] Raharjo RD, Freeman BD, Sanders ES. Pure and mixed gas CH<sub>4</sub> and *n*-C<sub>4</sub>H<sub>10</sub> sorption and dilation in poly(dimethylsiloxane). *Journal of Membrane Science* 2007;292:45–61.
- [34] Wijmans JG, Baker RW. The solution-diffusion model: a review. *Journal of Membrane Science* 1995;107:1–21.
- [35] Ghosal K, Freeman BD. Gas separation using polymer membranes: an overview. *Polymers for Advanced Technologies* 1994;5:673–97.
- [36] Petropoulos JH. In: Paul DR, Yampol'skii YP, editors. Boca Raton, FL: Polymeric gas separation membranes; 1994. p. 17–81.
- [37] Cohen MH, Turnbull D. Molecular transport in liquids and glasses. *Journal of Chemical Physics* 1959;31:1164–9.
- [38] Bondi A. van der Waals volumes and radii. *Journal of Physical Chemistry* 1964;68:441–51.
- [39] Bondi A. Physical properties of molecular crystals, liquids and glasses. New York: Wiley; 1968.
- [40] Van Krevelen DW. Properties of polymers. 3rd ed. Amsterdam: Elsevier; 2003.
- [41] Pinteala M, Harabagiu V, Simionescu BC, Guegan P, Cheradame H. Ionically conducting networks derived from PEO containing aziridine groups. *Polymer International* 1999;48:1147–54.
- [42] Treushnikov VM, Telepneva TV, Oleinik AV, Sorin EL, Korshak VV, Krongauz ES, et al. Photochemical crosslinking of poly(phenylquinoxalines) with aromatic azides. *Vysokomolekulyarnye Soedineniya, Seriya A* 1986;28:2129–34.
- [43] Yan M, Cai SX, Wybourne MN, Keana JFW. Evaluation of bis(perfluorophenyl azide)s as cross-linkers for a soluble polyimide. *Journal of Materials Chemistry* 1996;6:1249–52.
- [44] Yasuda N, Yamamoto S, Adachi H, Nagae S, Wada Y, Yanagida S. A novel photosensitive silicone ladder polymer: synthesis, photochemical, and thermal characteristics. *Bulletin of the Chemical Society of Japan* 2001;74:991–6.
- [45] Yasuda N, Yamamoto S, Wada Y, Yanagida S. Photocrosslinking reaction of vinyl-functional polyphenylsilsesquioxane sensitized with aromatic bisazide compounds. *Journal of Polymer Science Part A: Polymer Chemistry* 2001;39:4196–205.
- [46] CAB-O-SIL TS-530 Treated Fumed Silica. Technical Data, Cabot Corp.; 1991.
- [47] De Sitter K, Winberg P, D'Haen J, Dotremont C, Leysen R, Martens JA, et al. Silica filled poly(1-trimethylsilyl-1-propyne) nanocomposite membranes: relation between the transport of gases and structural characteristics. *Journal of Membrane Science* 2006;278:83–91.
- [48] Merkel TC, Freeman BD, Spontak RJ, He Z, Pinnau I, Meakin P, et al. Sorption, transport, and structural evidence for enhanced free volume in poly(4-methyl-2-pentyne)/fumed silica nanocomposite membranes. *Chemistry of Materials* 2003;15:109–23.
- [49] Ulutan S, Nakagawa T. Separability of ethanol and water mixtures through PTMSP-silica membranes in pervaporation. *Journal of Membrane Science* 1998;143:275–84.
- [50] Nagai K, Higuchi A, Nakagawa T. Gas permeability and stability of poly(1-trimethylsilyl-1-propyne-co-1-phenyl-1-propyne) membranes. *Journal of Polymer Science Part B: Polymer Physics* 1995;33:289–98.
- [51] Shimomura H, Nakanishi K, Odani H, Kurata M. Effects of physical aging on permeation of gases in a disubstituted polyacetylene. *Reports on Progress in Polymer Physics in Japan* 1987;30:233–6.
- [52] Ichiraku Y, Stern SA, Nakagawa T. An investigation of the high gas permeability of poly(1-trimethylsilyl-1-propyne). *Journal of Membrane Science* 1987;34:5–18.
- [53] Allcock H, Lampe F. Contemporary polymer chemistry. 2nd ed. London: Prentice-Hall; 1990.
- [54] Dean JA. Lange's handbook of chemistry. 15th ed. New York: McGraw-Hill; 1999.
- [55] Khodzhaeva VL, Zaikin VG, Khotimskii VS. Thermal oxidation of poly(1-trimethylsilylprop-1-yne) studied by IR spectroscopy. *Russian Chemical Bulletin* 2003;52:1333–9 (Translation of *Izvestiya Akademii Nauk, Seriya Khimicheskaya*).
- [56] Merkel TC, Bondar V, Nagai K, Freeman BD. Sorption and transport of hydrocarbon and perfluorocarbon gases in poly(1-trimethylsilyl-1-propyne). *Journal of Polymer Science Part B: Polymer Physics* 2000;38:273–96.
- [57] Robeson LM. Correlation of separation factor versus permeability for polymeric membranes. *Journal of Membrane Science* 1991;62:165–85.
- [58] Freeman BD. Basis of permeability/selectivity tradeoff relations in polymeric gas separation membranes. *Macromolecules* 1999;32:375–80.
- [59] Morisato A, Freeman BD, Pinnau I, Casillas CG. Pure hydrocarbon sorption properties of poly(1-trimethylsilyl-1-propyne) (PTMSP), poly(1-phenyl-1-propyne) (PPP), and PTMSP/PPP blends. *Journal of Polymer Science Part B: Polymer Physics* 1996;34:1925–34.
- [60] Breck DW. Zeolite molecular sieves: structure, chemistry, and use. New York: John Wiley & Sons; 1974. p. 553–724.
- [61] Merkel TC, Freeman BD, Spontak RJ, He Z, Pinnau I, Meakin P, et al. Ultraparpermeable, reverse-selective nanocomposite membranes. *Science* (Washington, DC, United States) 2002;296:519–22.
- [62] Pinnau I, He Z. Pure- and mixed-gas permeation properties of polydimethylsiloxane for hydrocarbon/methane and hydrocarbon/hydrogen separation. *Journal of Membrane Science* 2004;244:227–33.
- [63] Ash R, Barber RM, Pope CG. Flow of adsorbable gases and vapors in a microporous medium. II. Binary mixtures. *Proceedings of Royal Chemical Society (London)* 1963;271:19–33.
- [64] Rao MB, Sircar S. Nanoporous carbon membranes for separation of gas mixtures by selective surface flow. *Journal of Membrane Science* 1993;85:253–64.